Title

The p85 regulatory subunit of phosphoinositide 3-kinase down-regulates IRS-1 signaling via the formation of a sequestration complex

Journal

Journal of Cell Biology, 170(3)

ISSN

0021-9525

Authors

Luo, Ji
Field, Seth J
Lee, Jennifer Y
et al.

Publication Date

2005-08-01

DOI

10.1083/jcb.200503088

Peer reviewed

The p85 regulatory subunit of phosphoinositide 3-kinase down-regulates IRS-1 signaling via the formation of a sequestration complex

Ji Luo,[1,2] Seth J. Field,[1,2,3] Jennifer Y. Lee,[1,2] Jeffrey A. Engelman,[1,2,4] and Lewis C. Cantley[1,2]

[1]Department of Systems Biology, Harvard Medical School, and [2]Division of Signal Transduction, Beth Israel Deaconess Medical Center, Boston, MA 02115
[3]Division of Endocrinology and [4]Department of Hematology/Oncology, Massachusetts General Hospital, Boston, MA 02114

Phosphoinositide (PI) 3-kinase is required for most insulin and insulin-like growth factor (IGF) 1–dependent cellular responses. The p85 regulatory subunit of PI 3-kinase is required to mediate the insulin-dependent recruitment of PI 3-kinase to the plasma membrane, yet mice with reduced p85 expression have increased insulin sensitivity. To further understand the role of p85, we examined IGF-1–dependent translocation of p85α by using a green fluorescence protein (GFP)–tagged p85α (EGFP–p85α). In response to IGF-1, but not to PDGF signaling, EGFP–p85α translocates to discrete foci in the cell. These foci contain the insulin receptor substrate (IRS) 1 adaptor molecule, and their formation requires the binding of p85 to IRS-1. Surprisingly, monomeric p85 is preferentially localized to these foci compared with the p85–p110 dimer, and these foci are not sites of phosphatidylinositol-3,4,5-trisphosphate production. Ultrastructural analysis reveals that p85–IRS-1 foci are cytosolic protein complexes devoid of membrane. These results suggest a mechanism of signal down-regulation of IRS-1 that is mediated by monomeric p85 through the formation of a sequestration complex between p85 and IRS-1.

Introduction

In response to growth factors, class I_A phosphoinositide (PI) 3-kinases generate the phospholipid second messengers phosphatidylinositol-3,4,5-trisphosphate (PIP_3) and phosphatidylinositol-3,4-bisphosphate (PI-3,4-P_2; for review see Cantley, 2002). These lipids, in turn, activate a number of signaling molecules by binding to their pleckstrin homology (PH) domains. The serine–threonine protein kinase Akt is a major downstream target of PI 3-kinase. The PH domain of Akt specifically recognizes PIP_3 and PI-3,4-P_2 (James et al., 1996; Franke et al., 1997) upon recruitment to the plasma membrane, and Akt is activated by the phosphorylation of threonine-308 in its activation loop and by serine-473 at its COOH terminus (Alessi et al., 1997; for review see Chan and Tsichlis, 2001). Several lipid phosphatases, notably phosphatase and tensin homologue and SH2 domain–containing inositol phosphatase, act to rapidly degrade PIP_3 and, hence, terminate signaling through this pathway (Cantley and Neel, 1999; Rohrschneider et al., 2000).

Class I_A PI 3-kinase is a heterodimer consisting of a regulatory subunit (p85) and a catalytic subunit (p110). The p85 regulatory subunit stabilizes the p110 catalytic subunit and holds it in a low activity state (Yu et al., 1998b). The p85 regulatory subunit contains two Src homology (SH) 2 domains that recognize phosphotyrosine residues in the context pYxxM (pY, phosphotyrosine; x, any amino acid) on activated receptors or their adaptor molecules (Songyang et al., 1993). The binding of p85 to tyrosine-phosphorylated proteins serves both to relieve inhibition on the p110 catalytic subunit as well as to recruit PI 3-kinase from the cytosol to the plasma membrane, where its substrate, PI-4,5-P_2, resides (Rordorf-Nikolic et al., 1995). Mammals contain three different genes for the p85 regulatory subunit (p85α, p85β, and p55γ) and three different genes for the class I_A catalytic subunit (p110α, p110β, and p110δ). The major p85 isoform p85α also exists as two shorter splice variants (p55α and p50α) that lack the NH_2-terminal SH3 and RhoGAP homology domains of p85α (Fruman et al., 1998).

Both the insulin receptor and the highly homologous insulin-like growth factor (IGF) 1 receptor activate class I_A PI 3-kinase indirectly through phosphorylation of the insulin recep-

Correspondence to Lewis C. Cantley: lewis_cantley@hms.harvard.edu

S.J. Field's present address is Division of Endocrinology, Cellular and Molecular Medicine, University of California, San Diego, La Jolla, CA 92093.

Abbreviations used in this paper: IGF, insulin-like growth factor; IRS, insulin receptor substrate; MEF, mouse embryonic fibroblasts; PH, pleckstrin homology; PI, phosphoinositide; PIP_3, phosphatidylinositol-3,4,5-trisphosphate; PI-3,4-P_2, phosphatidylinositol-3,4-bisphosphate; SH, Src homology; TIRFM, total internal reflection fluorescence microscopy.

The online version of this article contains supplemental material.

The Journal of Cell Biology, Vol. 170, No. 3, August 1, 2005 455–464
http://www.jcb.org/cgi/doi/10.1083/jcb.200503088

tor substrate (IRS) family of adaptor molecules. These receptors phosphorylate tyrosine residues on IRS to create p85-binding sites (for review see Butler et al., 1998; Virkamaki et al., 1999). PI 3-kinase is a key mediator of metabolic signaling downstream of the insulin receptor, and it also mediates cell differentiation, survival, and proliferation downstream of both insulin and IGF-1 receptors (Dufourny et al., 1997; Kulik et al., 1997; Saltiel and Kahn, 2001; Tureckova et al., 2001). Despite the key role PI 3-kinase plays in mediating glucose uptake downstream of the insulin receptor, mice lacking various isoforms of the p85α or p85β subunit of PI 3-kinase demonstrated the paradoxical phenotype of increased insulin sensitivity, which was caused by improved PI 3-kinase signaling downstream of IRS proteins (Terauchi et al., 1999; Fruman et al., 2000; Mauvais-Jarvis et al., 2002; Ueki et al., 2002b; Chen et al., 2004). It was subsequently shown that the molecular balance between monomeric p85 and the p85–p110 dimer can influence the extent of PI 3-kinase signaling downstream of the insulin receptor, as monomeric p85 can negatively regulate PI 3-kinase signaling by competing with the p85–p110 dimer for IRS binding (Ueki et al., 2002a, 2003). Recently, it was also reported that the protein SOCS-6 can selectively bind to monomeric p85 and that overexpression of SOCS-6 improves insulin signaling in vivo (Li et al., 2004). Furthermore, the expression of the human placental hormone in transgenic mice results in the up-regulation of p85 and subsequent insulin resistance in muscle (Barbour et al., 2004). These lines of evidence suggest that monomeric p85 acts as a negative regulator of insulin signaling in vivo by controlling the extent of PI 3-kinase activation downstream of the receptor.

In this study, we have investigated the spatial translocation of the p85 regulatory subunit of PI 3-kinase in response to IGF-1 receptor activation. We find that 5–10 min after IGF-1 stimulation, p85 and IRS-1 assemble into large complexes (foci) in the cytosol. This complex formation appears to be driven preferentially by monomeric p85 rather than by p85–p110, and these complexes do not appear to be sites of PI-P_3 production. These results indicate a novel mechanism for limiting IRS-1/PI 3-kinase signaling that could explain why insulin/IGF-1 signaling is acutely sensitive to p85 levels.

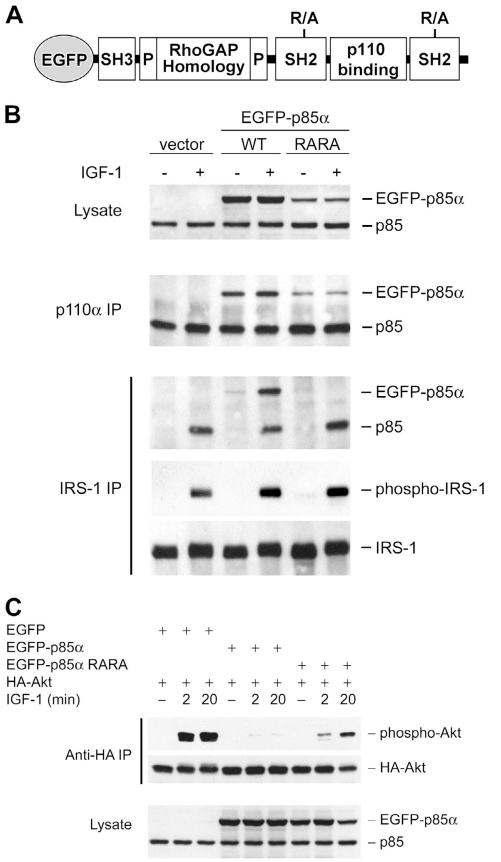

Figure 1. **Biochemical characterization of EGFP–p85α reporter constructs.** (A) Schematic representation of EGFP–p85α constructs with the domains illustrated (P, proline-rich region). EGFP was fused to the NH_2 terminus of p85α. The R/A (arginine to alanine) mutations in the conserved FLVRD/E motif of both SH2 domains of p85α are also indicated. (B) CHO-K1 cells transfected with either the wild-type EGFP–p85α or the SH2 domain mutant. EGFP–p85α RARA (which harbors the R358A and R649A point mutations in the SH2 domains) constructs were serum starved and stimulated with 10 nM IGF-1 for 10 min. The levels of EGFP–p85α and endogenous p85 in total cell lysate, p110α immunoprecipitate, and IRS-1 immunoprecipitate were probed with anti-p85 antibody. (C) CHO-K1 cells cotransfected with HA-Akt and EGFP–p85α or with HA-Akt and EGFP–p85α RARA were serum starved and stimulated with 10 nM IGF-1 for 2 or 20 min. Phosphorylation of HA-Akt was assessed by anti–phospho-Akt threonine-308 Western blot analysis of HA immunoprecipitate. Results shown are representative of two experiments.

Results

EGFP–p85α translocates to discrete foci in response to IGF-1 signaling

To explore the possibility that different growth factor receptors may result in the distinct spatial recruitment of PI 3-kinase, we generated an EGFP-tagged p85α chimera (EGFP–p85α; Fig. 1 A) that allowed us to visualize its localization in live cells using fluorescence video microscopy. When expressed in CHO-K1 cells at levels comparable with endogenous p85, this fusion protein behaved similarly to endogenous p85, as judged both by its ability to bind the p110 catalytic subunit and by its ability to bind tyrosine-phosphorylated IRS-1 adaptor protein after IGF-1 receptor activation (Fig. 1 B). Previous studies have shown that when overexpressed in cells, p85 inhibits PI 3-kinase signaling (Rameh et al., 1995; Ueki et al., 2000). In agreement with these studies, we found that the EGFP–p85α construct, when overexpressed in CHO-K1 cells at levels comparable with endogenous p85, significantly attenuated IGF-1–induced Akt activation (Fig. 1 C).

In serum-starved cells, EGFP–p85α localized diffusely in the cytoplasm and to membrane protrusions that have been attributed to focal adhesions in a previous study (Gillham et al., 1999). Because CHO-K1 cells express both IGF-1 and PDGF receptors endogenously, we first compared the recruitment of EGFP–p85α downstream of IGF-1 and PDGF receptors. Upon stimulation with IGF-1, EGFP–p85α was recruited to distinct foci within 5–10 min (Fig. 2 A and Video 1, available at http://www.jcb.org/cgi/content/full/jcb.200503088/DC1). Both low (1 nM) and high (20 nM) concentrations of IGF-1 induced the formation of EGFP–p85 foci in a similar fashion, although at the lower threshold of IGF-1 (1 nM), some cells failed to respond. Curiously, we did not observe significant global recruit-

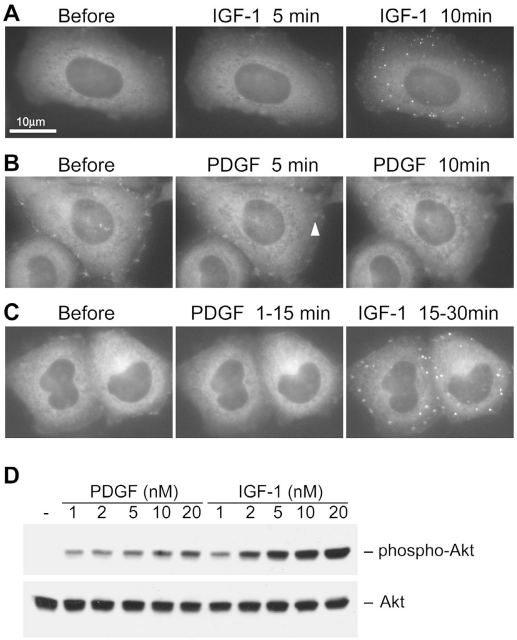

Figure 2. **IGF-1, but not PDGF, induces the translocation of EGFP–p85α to foci.** (A–C) CHO-K1 cells stably expressing EGFP–p85α were serum starved and stimulated with 1 nM IGF-1 (A), 20 nM PDGF (B), or first with 20 nM PDGF for 15 min followed by 1 nM IGF-1 for an additional 15 min (C). Cells were imaged live, and frames at indicated time points are shown. Arrowhead indicates PDGF-induced transient EGFP–p85α patches (Videos 1 and 2, available at http://www.jcb.org/cgi/content/full/jcb.200503088/DC1). Results shown are representative of at least five experiments. (D) CHO-K1 cells were serum starved and stimulated with either PDGF or IGF-1 at indicated concentrations for 10 min. Total cell lysates were probed with anti–phospho-Akt serine-473 antibody to assess the level of Akt activation. Results shown are representative of two experiments.

ment of EGFP–p85α to the plasma membrane in response to IGF-1 stimulation, suggesting that only a very small amount of p85 (and hence PI 3-kinase) may be present at the membrane at any given moment. On the other hand, PDGF stimulation resulted in transient, weak recruitment of EGFP–p85α to plasma membrane patches and ruffles (Fig. 2 B and Video 2, available at http://www.jcb.org/cgi/content/full/jcb.200503088/DC1). In addition, IGF-1 could induce EGFP–p85α foci formation in cells that were previously stimulated by high concentrations of PDGF (Fig. 2 C). This suggests that the activation of different growth factor receptors leads to a different spatial translocation of EGFP–p85α. Such differences in the spatial recruitment of EGFP–p85α are not simply a result of the difference in the signaling strength of these receptors. Using antibodies against phosphorylated Akt (i.e., activated Akt) as a readout for PI 3-kinase activation, we found that both IGF-1 and PDGF activated PI 3-kinase in these cells (Fig. 2 D). Furthermore, although PDGF at 20 nM activated PI 3-kinase more strongly than IGF-1 did at 1 nM, PDGF at 20 nM did not cause EGFP–p85α translocation to foci, whereas IGF-1 at 1 nM did.

We further explored the time course of IGF-1–dependent EGFP–p85α foci formation. EGFP–p85α foci were not detectable until 2–5 min after IGF-1 stimulation, and their fluorescence intensities reached maximum and stabilized within 10–20 min. In the continuous presence of IGF-1, these foci were stable structures that persisted in the cell, and, over time, some proceeded to fuse with each other (Fig. S1 B, available at http://www.jcb.org/cgi/content/full/jcb.200503088/DC1). On the other hand, withdrawing IGF-1 caused the majority of EGFP–p85α foci to disappear within 1 h (Fig. S1 C), suggesting that maintenance of the EGFP–p85α foci requires the presence of the activated IGF-1 receptor. The translocation of EGFP–p85α to foci downstream of IGF-1 receptors was not unique to CHO-K1 cells, as it was also observed in NIH3T3 cells (Fig. S2 A, available at http://www.jcb.org/cgi/content/full/jcb.200503088/DC1). Furthermore, a reporter construct for p85β (EYFP-p85β) demonstrated similar behavior to EGFP–p85α (Fig. S2 B). As EGFP itself can form weak dimers (for review see Zacharias, 2002), we also performed immunofluorescence staining against FLAG-tagged p85α and observed similar translocation within 20 min of IGF-1 stimulation (see Fig. 3 D). Therefore, the localization of EGFP–p85α to foci is not a result of EGFP moiety.

EGFP–p85α foci are complexes of p85 and tyrosine-phosphorylated IRS-1

Like the insulin receptor, the IGF-1 receptor activates PI 3-kinase through tyrosine phosphorylation of the IRS family of adaptor molecules, with IRS-1 being the best-characterized member (White, 1998). The pYxxM motifs on IRS-1 directly bind to the SH2 domains of p85 to recruit the p85–p110 complex (Backer et al., 1992; for review see Butler et al., 1998). Therefore, we tested whether the translocation of EGFP–p85α to foci that are downstream of the IGF-1 receptor requires its interaction with IRS-1. An arginine residue in the conserved FLVRD/E motif of the p85 SH2 domains is critical for coordinating the phosphate moiety of phosphotyrosine (Nolte et al., 1996). Mutations of this arginine to alanine in each of the p85 SH2 domains have been shown to abolish binding to phosphotyrosine without affecting their overall folding (Yu et al., 1998a). Thus, we introduced the same mutations (R358A and R649A in the FLVRD/E motif of each of the SH2 domains of p85α) to generate the EGFP–p85α RARA mutant. As expected, although this mutant bound the PI 3-kinase p110 catalytic subunit normally, it could no longer bind tyrosine-phosphorylated IRS-1 after IGF-1 stimulation (Fig. 1 B). Furthermore, the EGFP–p85α RARA mutant was much less effective at inhibiting Akt activation when overexpressed in cells (Fig. 1 C), indicating that functional SH2 domains are required for the inhibition of PI 3-kinase signaling by p85. When we coexpressed the CFP-tagged mutant ECFP-p85 RARA with the YFP-tagged wild-type EYFP-p85 in the same cell, only the wild-type EYFP-p85 translocated to foci in response to IGF-1, whereas the SH2 domain mutant ECFP-p85 RARA did not (Fig. 3 A). This indicates that the SH2 domains of p85 are essential in mediating such translocation.

Conversely, we asked whether IRS-1 is also present at the EGFP–p85α foci. Immunofluorescence staining against endogenous IRS-1 revealed that it colocalized to the EGFP–p85α foci after IGF-1 stimulation (Fig. 3 B). Interestingly, the localization of endogenous IRS-1 to foci was more prominent in cells that also expressed EGFP–p85α, suggesting that the modest amount of EGFP–p85α expressed in these cells promotes

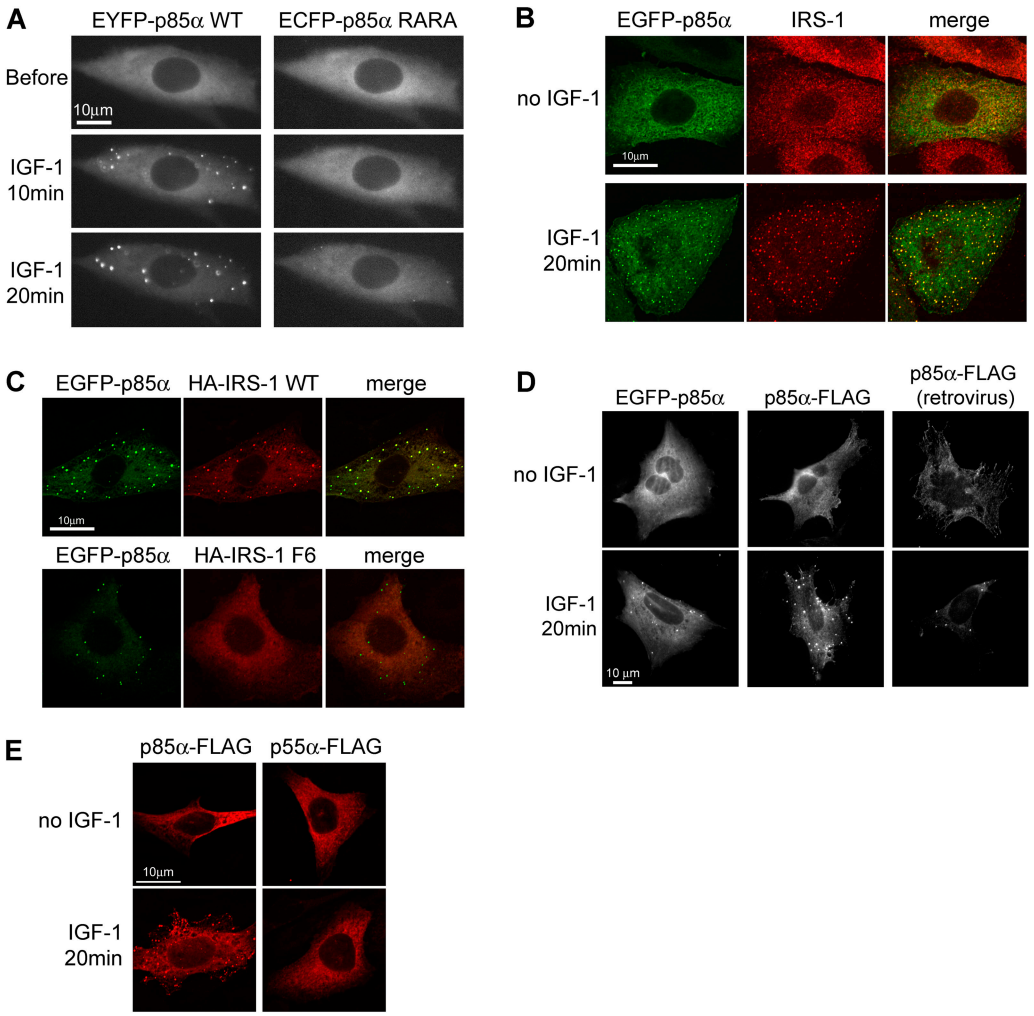

Figure 3. **EGFP–p85α foci consist of both p85α and IRS-1.** (A) CHO-K1 cells cotransfected with wild-type EYFP-p85 and SH2-domain mutant ECFP-p85 RARA were serum starved and stimulated with 10 nM IGF-1. Cells were imaged live in both the yellow and cyan fluorescence channels. Frames at the indicated time points are shown. (B) CHO-K1 cells stably expressing EGFP–p85α were serum starved and stimulated with 10 nM IGF-1 for 20 min. Cells were fixed, and endogenous IRS-1 was visualized with anti–IRS-1 immunofluorescence. (right) Merged image illustrates the colocalization of EGFP–p85α and anti–IRS-1 staining. (C) CHO-K1 cells cotransfected with EGFP–p85α and HA-tagged wild-type IRS-1 or mutant IRS-1–F6 constructs were serum starved and stimulated with 10 nM IGF-1 for 20 min. IRS-1 was visualized with anti-HA immunofluorescence. Results shown are representative of three experiments. (D) $p85\alpha^{-/-}p85\beta^{-/-}$ MEFs either transiently expressing EGFP–p85α (left) or p85α-FLAG (middle) or retrovirally expressing p85α-FLAG (right) were starved and stimulated with 10 nM IGF-1 for 20 min. Cells were fixed, and the localization of p85α was either directly visualized (EGFP–p85α) or was visualized by anti-FLAG immunofluorescence (p85α-FLAG). (E) CHO-K1 cells expressing FLAG-tagged p85α or p55α were serum starved and stimulated with 10 nM IGF-1 for 20 min. The localization of p85α-FLAG or p55α-FLAG was visualized by anti-FLAG immunofluorescence. Representative images of two experiments are shown.

the recruitment of IRS-1 to these foci. Tyrosine phosphorylation of IRS-1 is also critical for the localization of IRS-1 to these foci. When we coexpressed EGFP–p85α with a mutant IRS-1 that had six tyrosine residues mutated to phenylalanine (IRS-1–F6) and, hence, was impaired in PI 3-kinase binding (Esposito et al., 2001), this IRS-1–F6 mutant was also impaired in its ability to localize to EGFP–p85α foci (Fig. 3 C). These results suggest that tyrosine phosphorylation of IRS-1 and its binding to p85 is required for the recruitment of IRS-1 into these foci.

To rule out the possibility that only overexpressed p85α that is additional to endogenous p85 proteins can form such foci with IRS-1, we expressed EGFP–p85α and p85α-FLAG in mouse embryonic fibroblasts (MEFs) that were null for both the p85α and p85β genes (Brachmann et al., 2005b). We observed IGF-1–induced p85α foci formation in $p85\alpha^{-/-}p85\beta^{-/-}$ MEFs expressing even the lowest detectable levels of p85α proteins. Furthermore, the introduction of FLAG-tagged p85α into $p85\alpha^{-/-}p85\beta^{-/-}$ MEFs by retrovirus infection (using conditions that we have previously shown to result in exogenous p85α levels similar to or lower than endogenous p85α of wild-type MEFs; Brachmann et al., 2005b) led to p85α foci in response to IGF-1 (Fig. 3 D). Thus, p85α–IRS-1 foci appear in response to IGF-1 in cells in which total p85α is at or below endogenous levels.

Interestingly, we found that the shorter isoform p55α, which lacks the NH_2-terminal SH3 and RhoGAP homology domains of p85α, did not translocate to foci in response to IGF-1 (Fig. 3 E). A similar result was obtained with the other shorter isoform p50α (unpublished data). This suggests that SH3 and/

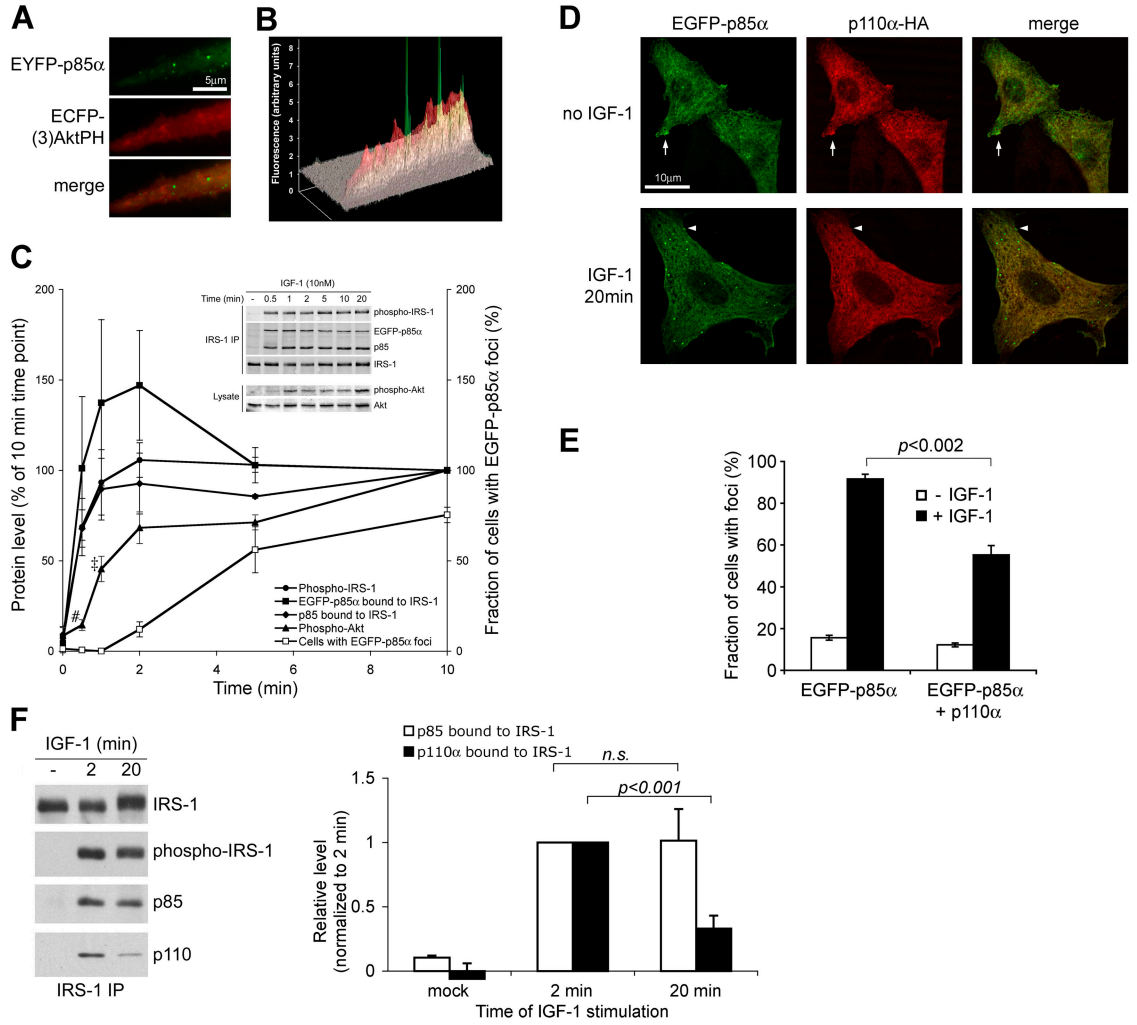

Figure 4. **EGFP–p85α foci are not the sites of PIP_3 production.** (A) CHO-K1 cells cotransfected with EYFP-p85α and ECFP-(3)AktPH constructs were serum starved and stimulated with 10 nM IGF-1. Cells were imaged live in both the yellow and cyan fluorescence channels. Frames at 10 min post–IGF-1 stimulation are shown. (B) The fluorescence intensity in A was profiled to show the lack of colocalization between the signal of EYFP-p85α (green) and that of ECFP-(3)AktPH (red). Results shown are representative of three experiments. (C) CHO-K1 cells stably expressing EGFP–p85α were serum starved and stimulated with 10 nM IGF-1 for the indicated periods of time. The levels of tyrosine-phosphorylated IRS-1, EGFP–p85α, and p85 that bound to IRS-1 and serine-473–phosphorylated Akt on Western blots were quantified and normalized to their respective levels at the 10-min time point. A representative blot is shown in the inset. At each time point, the percentage of cells that harbor EGFP–p85α foci were also counted. Data represent mean ± SEM of three experiments (#, $P < 0.01$; ‡, $P < 0.08$; compared with IRS-1–bound p85 levels at the same time point). (D) CHO-K1 cells cotransfected with EGFP–p85α and HA-tagged p110α were serum starved and stimulated with 10 nM IGF-1 for 20 min. p110α was visualized with anti-HA immunofluorescence. The right panel shows the merged image. Arrow, focal adhesion-like structure; arrowhead, EGFP–p85α focus. Results shown are representative of three experiments. (E) CHO-K1 cells transfected with EGFP–p85α alone or with EGFP–p85α and HA-tagged p110α were serum starved and stimulated with 10 nM IGF-1 for 20 min. The number of transfected cells that also contained EGFP–p85α foci were counted. Results shown are mean ± SEM from three experiments. (F) CHO-K1 cells were serum starved and stimulated with 10 nM IGF-1 for either 2 or 20 min. The levels of endogenous p85 and p110α in IRS-1 immunoprecipitate were assessed by Western blotting (left) and quantified by densitometry (right). The relative levels of p85 and p110α at each time point was calculated by normalizing against their respective values at the 2-min time point. Results shown are mean ± SEM from three experiments.

or RhoGAP homology domains of p85α play a role in its localization to these foci.

EGFP-p85α–IRS-1 complexes are sites of IRS-1 sequestration

We next investigated whether these EGFP–p85α–IRS-1 foci are sites of PIP_3 production. We first used Akt–PH domain–EGFP fusion protein as a reporter to detect PIP_3 production in the cell (Gray et al., 1999). We were able to improve the sensitivity of this reporter by trimerizing the PH domain (EGFP-[3]AktPH). As expected, EGFP-(3)AktPH translocated to the plasma membrane in response to stimulation by growth factors, whereas an analogous construct bearing an R25C mutation in each of the PH domains that abolishes binding to the 3′ phosphate of PIP_3 (Varnai et al., 1999) failed to do so (Fig. S3, available at http://www.jcb.org/cgi/content/full/jcb.200503088/DC1). In addition, the membrane translocation of EGFP-(3)AktPH was also blocked by the PI 3-kinase inhibitor wortmannin (unpublished data). After IGF-1 stimulation, EGFP-(3)AktPH consistently translocated to plasma membrane patches and ruffles within 1–2 min, which is a time course that is more rapid than that of the EGFP–p85α translocation to foci. The pattern of Akt PH domain localization was much more diffused than that of the EGFP–p85α foci (Fig. S3).

When EYFP-p85α and ECFP-(3)AktPH were coexpressed in the same cell and imaged simultaneously, the translocation of the ECFP-(3)AktPH domain to the plasma membrane was often found to be suppressed (unpublished data), again indicating the down-regulation of PI 3-kinase signaling by p85. In cells in which ECFP-(3)AktPH did show detectable membrane translocation, ECFP-(3)AktPH patches did not colocalize with the EYFP-p85α foci (Fig. 4, A and B), suggesting that these EYFP-p85α foci are not the sites of PIP_3 production. This conclusion is further supported by the observation that IRS-1 phosphorylation, PI 3-kinase activation, and Akt activation precedes the appearance of EGFP–p85α foci in CHO-K1 cells. As shown in Fig. 4 C, ~90% of maximum tyrosine phosphorylation on IRS-1 occurred within the first minute after IGF-1 stimulation. The recruitment of PI 3-kinase to IRS-1 was equally rapid with a nearly identical time course. It took ~2 min, however, for the majority of Akt to become activated; this short delay presumably reflects the time required for PI 3-kinase to generate PIP_3 at the plasma membrane. Furthermore, there was an ~5-min delay before most cells were observed to harbor EGFP–p85α foci. The activation of Akt, therefore, precedes the formation of EGFP–p85α foci.

Direct localization of the p110 catalytic subunit of PI 3-kinase by using a COOH-terminal HA-tagged p110α gave us a surprising result: although it colocalized with EGFP–p85α to focal adhesion-like structures in quiescent cells, it did not colocalize to the EGFP–p85α foci after IGF-1 stimulation (Fig. 4 D). This result suggests that only free, monomeric p85α, but not p110-bound p85α, is able to translocate to the foci. Indeed, the fraction of cells harboring EGFP–p85α foci upon IGF-1 stimulation was reduced from 90 to 60% when p110α was coexpressed with EGFP–p85α (Fig. 4 E). This result also explains the observation that the localization of IRS-1 to foci is more prominent in cells expressing EGFP–p85, presumably because even modest overexpression of EGFP–p85α significantly increases the relative level of p85 monomer to p85–p110 dimer. Altogether, these results suggest that EGFP–p85α foci contain primarily monomeric p85 but not p85–p110 dimer, and that they are not a site of PI 3-kinase signaling. These observations suggest that p85–IRS-1 foci may actually serve to down-regulate PI 3-kinase signaling by sequestering tyrosine-phosphorylated IRS-1 and, hence, limit its recruitment of the p85–p110 dimer. Indeed, when we assessed the amount of endogenous p85 and p110 that is associated with IRS-1 at either 2 min (before foci formation) or 20 min (after foci formed) after IGF-1 stimulation, we found that the level of IRS-1–bound p110α at 20 min post–IGF-1 stimulation was only 33% of that at 2 min. In contrast, the levels of IRS-1–bound p85 remained essentially unchanged (Fig. 4 F). Thus, the molecular balance between IRS-1–associated p110 and p85 has shifted from the p85–p110 dimer to the p85 monomer with a time frame comparable with that of EGFP–p85α–IRS-1 foci formation.

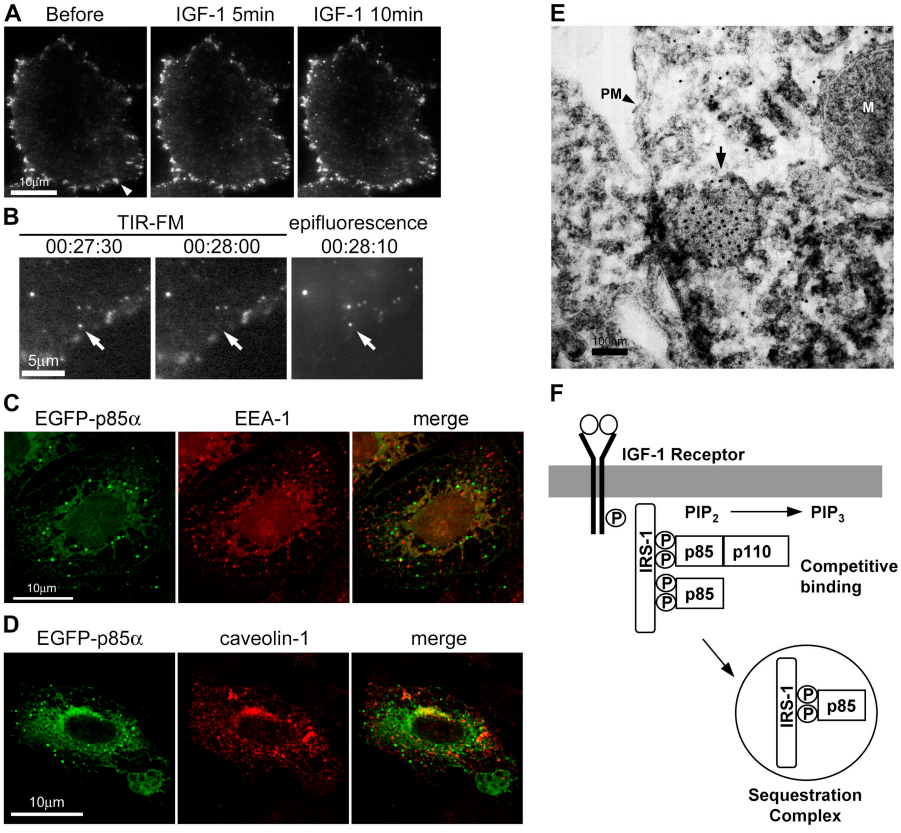

Figure 5. **EGFP–p85α foci are intracellular protein complexes.** (A) CHO-K1 cells stably expressing EGFP–p85α were serum starved and stimulated with 10 nM IGF-1. Cells were imaged live under TIRFM, and frames of the indicated time points are shown. Arrowhead, focal adhesion-like structure. Results shown are representative of three experiments. (B) Same experiment as in A; the internalization of one of the EGFP–p85α foci (arrow) away from the field of view of TIRFM was captured at the indicated time frames. Thereafter, the illumination was immediately switched from TIRFM to epifluorescence to show that the same spot was still visible under epifluorescence microscopy. (C) CHO-K1 cells stably expressing EGFP–p85α were serum starved and stimulated with IGF-1 for 60 min. Endogenous EEA1 protein was visualized with anti-EEA1 immunofluorescence. Similar results were obtained when cells were stimulated with IGF-1 for 10 or 30 min. Results shown are representative of three experiments. (D) CHO-K1 cells stably expressing EGFP–p85α were serum starved and stimulated with IGF-1 for 10 min. Endogenous caveolin-1 protein was visualized with anti–caveolin-1 immunofluorescence. Similar results were obtained when cells were stimulated with IGF-1 for 30 or 60 min. Results shown are representative of three experiments. (E) CHO-K1 cells stably expressing EGFP–p85α were serum starved and stimulated with IGF-1 for 20 min. EGFP–p85α was immunogold stained and visualized with transmission EM (PM, plasma membrane; M, mitochondrion; arrow, one EGFP–p85α focus). (F) A proposed model of the sequestration of IRS-1 by monomeric p85 as a means to negatively regulate PI 3-kinase signaling. P, phosphorylation on tyrosine residues.

EGFP–p85α–IRS-1 complexes are cytosolic protein complexes

Previous studies in 3T3-L1 cells have suggested that IRS-1 and p85 are selectively enriched in intracellular membrane fractions after insulin stimulation (Nave et al., 1996; Inoue et al., 1998). To determine the subcellular localization and structural nature of EGFP–p85α foci, we first assessed their membrane proximity with total internal reflection fluorescence microscopy (TIRFM) to visualize EGFP–p85α that was within ~100 nm of the plasma membrane (Toomre and Manstein, 2001). Interestingly, as with epifluorescence microscopy, we did not observe prominent global translocation of EGFP–p85α to the plasma membrane upon IGF-1 stimulation. TIRFM revealed that many of the EGFP–p85α foci formed near the plasma membrane (Fig. 5 A and Video 3, available at http://www.jcb.org/cgi/content/full/jcb.200503088/DC1). Once formed, however, many foci internalized away from the plasma membrane as they became invisible under TIRFM, whereas they were still visible under epifluorescence microscopy (Fig. 5 B).

Signaling through the IGF-1 receptor (as well as through the insulin receptor) has been shown to be regulated by endocytosis via clathrin-coated vesicles as well as by caveolae (Chow et al., 1998; Rotem-Yehudar et al., 2001; Huo et al., 2003). Our observations that EGFP–p85α foci were not the sites of PIP_3 production and could internalize away from the plasma membrane suggest that such foci may be endocytotic vesicles, which prompted us to examine whether EGFP–p85α foci represent either early endosomes or caveolae. Immunofluorescence staining revealed that EGFP–p85α foci did not colocalize with the early endosome marker EEA1 even after extended incubation with IGF-1 (Fig. 5 C). Similarly, using immunofluorescence staining against caveolin-1 as a marker for caveolae, we found that EGFP–p85α foci also did not colocalize with caveolin-1 (Fig. 5 D). Both the actin cytoskeleton and PI 3-kinase itself have been implicated in the regulation of endocytosis and endosomal trafficking (Joly et al., 1995; Engqvist-Goldstein and Drubin, 2003). Neither the PI 3-kinase inhibitor wortmannin nor the actin-depolymerizing agent latrunculin B or the microtubule-destabilizing agent nocodazole, however, had any effect on the formation of EGFP–p85α foci (unpublished data). Thus, these results indicate that EGFP–p85α foci are unlikely to be endocytotic vesicles. Next, we determined the ultrastructure of EGFP–p85α foci by immunogold EM. In unstimulated cells, immunogold staining against EGFP–p85α was diffuse in the cytoplasm (unpublished data). In IGF-1–stimulated cells, clusters of staining were observed in electron-dense structures 100–200 nm in diameter that resided in the cytoplasm (Fig. 5 E). These structures are likely to be protein complexes rather than vesicles because they were not delimited with lipid bilayers and there was no exclusion of staining from the center of these structures.

Discussion

The p85 regulatory subunit of class I_A PI 3-kinase is essential for both the stability of the p110 catalytic subunit (Yu et al., 1998a,b) and its recruitment to activated growth factor receptors or adaptor molecules (Cantley, 2002). Therefore, it was a surprise that mice lacking the various p85 regulatory subunits actually showed improved insulin signaling and enhanced insulin-stimulated Akt activation (Terauchi et al., 1999; Fruman et al., 2000; Ueki et al., 2002b; Chen et al., 2004). This paradox was, in part, reconciled by the observation that the p85 regulatory subunit is in excess over the p110 catalytic subunit in many cell types and that monomeric p85 competes with p85–p110 heterodimers for binding to IRS proteins (Ueki et al., 2002a,b, 2003; Brachmann et al., 2005a). This competitive binding model (Fig. 5 F) could explain why deleting a subset of p85 regulatory genes (homozygous deletion of p85β, heterozygous deletion of p85α, or deletion of specific alternative splice variants of p85α), which leads to reduced levels of monomeric p85 with little effect on p85–p110 heterodimers, ultimately results in enhanced binding of p85–p110 PI 3-kinase to IRS proteins and increased insulin sensitivity (Mauvais-Jarvis et al., 2002; Ueki et al., 2002b; Chen et al., 2004). However, this model fails to explain why the homozygous deletion of all splice variants of p85α also results in increased insulin sensitivity (Fruman et al., 2000). Insulin-sensitive tissues from these mice have dramatically lower levels of PI 3-kinase activity as a result of a reduction in all forms of class I_A p85–p110 enzymes. As a consequence, less PI 3-kinase activity is recruited to IRS proteins 5 min after insulin stimulation. However, glucose clearance from the serum is dramatically enhanced, and serum insulin levels are lower. These results indicate that monomeric p85 protein plays a negative role in insulin signaling that is more complex than simple competition with p85–p110 for binding to IRS-1.

In the current study, by using EGFP–p85α as a reporter for the localization of p85 in live cells, we found that IGF-1 receptor activation induces the translocation of EGFP–p85α to distinct, foci-like complexes that contain p85 bound to tyrosine-phosphorylated IRS-1 (Figs. 2 and 3). The interaction between p85 and IRS-1 is critical for the dominant negative effect of monomeric p85, as the SH2 domain–mutated p85 that fails to bind IRS-1 and form foci is far less effective at inhibiting PI 3-kinase signaling (Fig. 1, B and C). Surprisingly, these complexes contain primarily monomeric p85 with less of the p85–p110 dimer and appear to be protein-only complexes that are devoid of membrane components. Because these complexes are not on the membrane, the enzyme would not have access to its lipid substrate even if some p85–p110 dimer was present in the complex (Figs. 4 and 5). These observations suggest a novel mechanism to explain how monomeric p85 inhibits PI 3-kinase signaling downstream of IRS-1 (Fig. 5 F). In this modified model, in addition to being a competitive inhibitor for p85–p110 binding to IRS-1, monomeric p85 sequesters IRS-1 in cytosolic protein complexes and renders it incapable of stimulating PIP_3 production. The failure to form these sequestration complexes in mice lacking all isoforms of p85α (Fruman et al., 2000) would explain why insulin signaling in these animals is more efficient even though less PI 3-kinase is present. As the absence of monomeric p85 would eliminate the sequestration of IRS-1, this allows the small amount of p85–p110 dimers that form complexes with IRS-1 to efficiently signal for a longer period of time.

The two mechanisms of negative regulation by monomeric p85 (competitive binding vs. sequestration) are likely to operate in concert to limit both the amplitude and duration of PI 3-kinase signaling downstream of IRS-1. The competitive binding of monomeric p85 for IRS-1 modulates the amplitude of PI 3-kinase signaling at early time points (e.g., 1–2 min) after IGF-1 stimulation, whereas the sequestration of IRS-1 by p85 in a nonsignaling complex at later time points (10–20 min) serves to limit the duration (and possibly the overall amplitude) of PI 3-kinase signaling. In comparison to the competitive binding model, the sequestration model displays two additional properties that make it an attractive mechanism for signal down-regulation. First, the formation of the p85–IRS-1 complex occurs with a 5–10-min time delay (Fig. S1 A), thus allowing IRS-1 a short window of time to recruit and activate p85–p110 PI 3-kinase (which occurs within 1 min of receptor ligation; Fig. 4 C); thereafter, the sequestration of IRS-1 would rapidly attenuate the signal. Furthermore, as the p85–IRS-1 complexes persist for an extended period of time after IGF-1 withdrawal (30 min–1 h; Fig. S1 C), they could also serve as a mechanism of recalcitrance to subsequent IGF-1 or insulin stimulation. Second, the sequestration model provides a mechanism by which a small amount of monomeric p85 could have a profound impact on PI 3-kinase signaling, as a relatively small change in the monomeric p85 level could lead to a relatively large change in the amount of tyrosine-phosphorylated IRS-1 that is available to recruit the p85–p110 dimer.

Existing antibodies to p85 localize to foci-like structures in a number of cell types. However, these antibodies also detect foci-like structures in $p85\alpha^{-/-}p85\beta^{-/-}$ fibroblasts, hence precluding their specificity towards p85 in immunofluorescence staining. Although we were unable to identify a p85 antibody that was suitable for the localization of endogenous p85 by immunofluorescence, it is likely that endogenous, monomeric p85 also forms sequestration complexes with IRS-1 in response to IGF-1 or insulin signaling. Low levels of p85α expression alone in $p85\alpha^{-/-}p85\beta^{-/-}$ MEFs that completely lacked endogenous p85 proteins were sufficient for IGF-1–induced p85α–IRS-1 foci (Fig. 3 D), suggesting that such complex formation can occur at p85 levels close to that of endogenous p85 proteins. Our biochemical analysis of the levels of IRS-1–associated endogenous p85 and p110 reveals that there is far less p110 associated with IRS-1 at 20 min post-stimulation compared with that at 2 min, whereas the amount of p85 that is associated with IRS-1 remains essentially unchanged at these time points (Fig. 4 F). The IRS-1–associated p85/p110 ratio, therefore, shifts toward p85 at a later time (20 min post–IGF-1 stimulation) and in temporal correlation with the appearance of p85–IRS-1 complexes. Consistent with this model, the elevation of in vivo p85 levels (with no change in p110 levels) occurs in response to placental growth hormone, which has been shown to correlate with pregnancy-induced insulin resistance (Barbour et al., 2004; Kirwan et al., 2004). Thus, the changes in insulin or IGF-1 sensitivity that we observed upon manipulation of the levels of p85 isoforms in mice or in cell lines are in agreement with pathophysiological insulin resistance that occurs in correlation with the elevation of p85 levels in vivo.

Finally, it is of interest to note that only the full-length isoforms of p85 (p85α and p85β), but not the shorter isoforms (p55α and p50α), could form complexes with IRS-1 (Fig. 3 D), albeit p55α and p50α possess the same SH2 domains as p85α. This suggests that in addition to the SH2 domains, the NH_2-terminal half of p85 is also necessary for the formation of the p85–IRS-1 complex. It has been shown that p85 can homodimerize through its NH_2-terminal SH3 and RhoGAP homology domains (Harpur et al., 1999). This observation provides an intriguing mechanism of p85–IRS-1 complex formation. A p85 homodimer would have four SH2 domains available (two on each p85 monomer) that could, in theory, bind to various combinations of at least six phosphotyrosine motifs on IRS-1. Thus, a given p85 homodimer could bind to two or more distinct IRS-1 molecules and vice versa. This would allow the multimerization of p85 and IRS-1 that leads to the formation of a large globular structure, which is consistent with the EM image of the p85–IRS-1 complex (Fig. 5 E). Alternatively, other molecules that interact with the NH_2-terminal half of p85 may be required for the formation of the p85–IRS-1 sequestration complex.

In conclusion, we demonstrate in this study that the p85 regulatory subunit of PI 3-kinase, when in excess over the p110 catalytic subunit, can drive the formation of large complexes that contain tyrosine-phosphorylated IRS-1 after IGF-1 receptor ligation. The p85–IRS-1 complex localizes to the cytosol and, thus, is not a site for PI-3,4,5-P_3 production. We propose that the formation of this complex provides a mechanism for limiting insulin and IGF-1 signaling in vivo. It also offers an explanation for why the elevation of p85 under pathophysiological conditions correlates with insulin resistance, whereas the deletion of p85 genes results in increased insulin sensitivity even under conditions in which total PI 3-kinase activity is reduced.

Materials and methods

Plasmids, cell culture, antibodies, and other reagents

Mouse full-length p85α and p85β cDNA were PCR cloned into EGFP/EYFP/ECFP-C1 vectors (CLONTECH Laboratories, Inc.) to create the GFP/YFP/CFP-tagged p85 constructs. p85α constructs also carry a FLAG tag at its COOH terminus. The R358A and R649A mutations in p85α were generated by sequential site-directed PCR mutagenesis. The EGFP–p85α fragment was excised from the EGFP-C1-p85α plasmid and was subcloned into the ecdysone-inducible pFR-MCS vector (R. Herzig, RHeoGene) to generate pFR-MCS-EGFP–p85α. COOH-terminally tagged p85α and p55α were generated by subcloning mouse p85α and p50α into the pCMV6 vector. Retrovirus expressing tagged p85α was generated from a p85α-FLAG construct in pJP1520 retroviral vector. COOH-terminally HA-tagged p110 was generated by PCR cloning of bovine p110α into pcDNA3 vector. Human Akt1 PH domain (aa 1–164) was PCR cloned into EGFP/EYFP/ECFP-N1 vectors (CLONTECH Laboratories, Inc.) to create the GFP/YFP/CFP-tagged Akt PH domain constructs. The R25C mutation in the Akt PH domain was generated by site-directed PCR mutagenesis. Multimerized Akt PH domain constructs were created by the insertion of additional copies of the PH domains into the single Akt PH domain construct. The plasmids pCIS2–IRS-1 and pCIS2–IRS-1–F6, which express HA-tagged wild-type or mutant human IRS-1, respectively, were a gift from M.J. Quon (National Institutes of Health [NIH], Bethesda, MD).

CHO-K1 cells were maintained in DME-F12 and 10% FCS with 10% CO_2, whereas $p85\alpha^{-/-}p85\beta^{-/-}$ MEFs were maintained in DME and 15% FCS with 10% CO_2. Transient transfection was performed using LipofectAMINE Plus (Invitrogen). Stable CHO-K1 cells expressing EGFP–p85α under an ecdysone-inducible promoter were established by serial transfection of the cells first with the plasmids pEcR, pRXR, and pTK-hyg, and then with the plasmids pSV40/Zeo2 and pFR-MCS-EGFP–p85 (RHeoGene).

Stable clones were screened for the inducible expression of EGFP–p85α in response to the ecdysone analogue GS-E and were maintained in DME-F12 and 10% FCS supplemented with 350 μg/ml hygromycin (GIBCO BRL) and 400 μg/ml Zeocin (Invitrogen). The expression of EGFP–p85α was induced with 5 μM GS-E for 24–48 h.

Anti-p85 and anti-pTyr antibodies have been described previously (Fruman et al., 2000). Anti–IRS-1 and anti-p110α antibodies were obtained from Upstate Biotechnology; anti-EEA1 and anti–caveolin-1 antibodies were from Transduction Laboratories; anti–phospho-Akt serine-473, anti–phospho-Akt threonine-308, and anti-Akt antibodies were from Cell Signaling Technology; anti-HA antibody was from Sigma-Aldrich; anti-EGFP antibody was from CLONTECH Laboratories, Inc.; Texas red–conjugated secondary antibodies were from Jackson ImmunoResearch Laboratories; and colloidal gold-conjugated secondary antibody was from Utrecht University Medical Center. IGF-1 and PDGF were from Austral Biologicals.

Protein immunoblotting, immunoprecipitation, and immunostaining

Cells were lysed in lysis buffer (25 mM Tris-HCl, pH 7.4, 150 mM NaCl, 10% glycerol, 1% NP-40, 1 mM EDTA, 1 mM DTT, 20 mM NaF, 10 mM sodium pyrophosphate, 50 mM β-glycerophosphate, 1 mM Na_3VO_4, 1 mM PMSF, and 4 μg/ml each of leupeptin, aproteinin, and pepstatin). Clarified lysate was subjected to immunoprecipitation overnight at 4°C, and the immunoprecipitate was washed three times with wash buffer (25 mM Tris-HCl, pH 7.4, 150 mM NaCl, 1 mM EDTA, 20 mM NaF, 10 mM sodium pyrophosphate, and 50 mM β-glycerophosphate). Proteins were separated on SDS-PAGE gels and subjected to Western blotting. Quantitation of the Western signal was performed using an imaging system (Odyssey; LI-COR Biosciences). Immunofluorescence staining was essentially the same as described previously (Kanai et al., 2001), as was immunogold staining for EM (Griffiths, 1993).

Microscopy

For live cell imaging experiments, cells were maintained in phenol red–free DME-F12 in an environment chamber on a 37°C heated microscope stage. A 10% CO_2 environment was also applied for imaging experiments exceeding 1 h. IGF-1 or PDGF was directly added to the environment chamber to achieve the desired final concentrations. Ligand was removed with acid wash in some experiments (Jones and Kazlauskas, 2001). Live cell epifluorescence video microscopy was performed on a microscope (Diaphot 300; Nikon) with filter sets for EGFP, EYFP, and ECFP fluorescence using a 60× oil immersion objective or a 20× objective, and images were captured with ImagePro 4 software (Media Cybernetics). Live cell TIRFM was performed on a modified microscope (model IX70; Olympus) with a single green laser using a 60× oil immersion objective, and images were captured with Metamorph 5 software (Universal Imaging Corp.). Immunofluorescence imaging of fixed cells was performed on a confocal microscope (model E800; Nikon/Bio-Rad Laboratories) with a dual green/red laser using a 100× oil immersion objective, and images were captured with LaserSharp 2000 software (Bio-Rad Laboratories). Immunogold transmission EM was performed on an electron microscope (model 1200EX; JEOL). Raw images were further processed by using Adobe Photoshop 7 for presentation, and, in some cases, brightness and contrast were adjusted linearly and consistently for all images within the same experiment. Videos were compiled and annotated by using QuickTime Pro software (Apple Computer, Inc.).

Online supplemental material

Fig. S1 shows the dynamics of EGFP–p85α foci in CHO-K1 cells after IGF-1 stimulation and the subsequent removal of IGF-1. Fig. S2 shows EGFP–p85α foci formation in NIH3T3 cells and EYFP-p85β foci formation in CHO-K1 cells after IGF-1 stimulation. Fig. S3 shows translocation of the EGFP-(3)AktPH reporter construct in response to IGF-1 stimulation in CHO-K1 cells. Videos 1–3 are time-lapse videos of CHO-K1 cells expressing EGFP–p85α that are stimulated with either IGF-1 or PDGF. Selected frames of these videos are shown in Figs. 2 (A and B) and 5 A, respectively.

We thank Dr. Ron Herzig and Dr. Michael Quon for providing us with plasmids and DNA constructs, Vassilious Bezzerides and Dr. David Clapham for assistance with TIRFM, Maria Ericcson for assistance with EM, and Dr. John Blenis, Dr. Thomas Roberts, and Dr. Junying Yuan for discussion and advice.

This work was supported by a Howard Hughes Medical Institute (HHMI) Predoctoral Fellowship to J. Luo, by an HHMI Physician Postdoctoral Fellowship and an NIH grant (K08 DK065108-01) to S.J. Field, and by NIH grants (GM41890 and CA089021) to L.C. Cantley.

Submitted: 16 March 2005
Accepted: 20 June 2005

References

Alessi, D.R., S.R. James, C.P. Downes, A.B. Holmes, P.R. Gaffney, C.B. Reese, and P. Cohen. 1997. Characterization of a 3-phosphoinositide-dependent protein kinase which phosphorylates and activates protein kinase Balpha. *Curr. Biol.* 7:261–269.

Backer, J.M., M.G. Myers Jr., S.E. Shoelson, D.J. Chin, X.J. Sun, M. Miralpeix, P. Hu, B. Margolis, E.Y. Skolnik, J. Schlessinger, et al. 1992. Phosphatidylinositol 3′-kinase is activated by association with IRS-1 during insulin stimulation. *EMBO J.* 11:3469–3479.

Barbour, L.A., J. Shao, L. Qiao, W. Leitner, M. Anderson, J.E. Friedman, and B. Draznin. 2004. Human placental growth hormone increases expression of the p85 regulatory unit of phosphatidylinositol 3-kinase and triggers severe insulin resistance in skeletal muscle. *Endocrinology.* 145:1144–1150.

Brachmann, S.M., K. Ueki, J.A. Engelman, R.C. Kahn, and L.C. Cantley. 2005a. Phosphoinositide 3-kinase catalytic subunit deletion and regulatory subunit deletion have opposite effects on insulin sensitivity in mice. *Mol. Cell. Biol.* 25:1596–1607.

Brachmann, S.M., C.M. Yballe, M. Innocenti, J.A. Deane, D.A. Fruman, S.M. Thomas, and L.C. Cantley. 2005b. Role of phosphoinositide 3-kinase regulatory isoforms in development and actin rearrangement. *Mol. Cell. Biol.* 25:2593–2606.

Butler, A.A., S. Yakar, I.H. Gewolb, M. Karas, Y. Okubo, and D. LeRoith. 1998. Insulin-like growth factor-I receptor signal transduction: at the interface between physiology and cell biology. *Comp. Biochem. Physiol. B Biochem. Mol. Biol.* 121:19–26.

Cantley, L.C. 2002. The phosphoinositide 3-kinase pathway. *Science.* 296: 1655–1657.

Cantley, L.C., and B.G. Neel. 1999. New insights into tumor suppression: PTEN suppresses tumor formation by restraining the phosphoinositide 3-kinase/AKT pathway. *Proc. Natl. Acad. Sci. USA.* 96:4240–4245.

Chan, T.O., and P.N. Tsichlis. 2001. PDK2: a complex tail in one Akt. *Sci. STKE.* 10.1126/stke.2001.66.pe1.

Chen, D., F. Mauvais-Jarvis, M. Bluher, S.J. Fisher, A. Jozsi, L.J. Goodyear, K. Ueki, and C.R. Kahn. 2004. p50alpha/p55alpha phosphoinositide 3-kinase knockout mice exhibit enhanced insulin sensitivity. *Mol. Cell. Biol.* 24:320–329.

Chow, J.C., G. Condorelli, and R.J. Smith. 1998. Insulin-like growth factor-I receptor internalization regulates signaling via the Shc/mitogen-activated protein kinase pathway, but not the insulin receptor substrate-1 pathway. *J. Biol. Chem.* 273:4672–4680.

Dufourny, B., J. Alblas, H.A. van Teeffelen, F.M. van Schaik, B. van der Burg, P.H. Steenbergh, and J.S. Sussenbach. 1997. Mitogenic signaling of insulin-like growth factor I in MCF-7 human breast cancer cells requires phosphatidylinositol 3-kinase and is independent of mitogen-activated protein kinase. *J. Biol. Chem.* 272:31163–31171.

Engqvist-Goldstein, A.E., and D.G. Drubin. 2003. Actin assembly and endocytosis: from yeast to mammals. *Annu. Rev. Cell Dev. Biol.* 19:287–332.

Esposito, D.L., Y. Li, A. Cama, and M.J. Quon. 2001. Tyr(612) and Tyr(632) in human insulin receptor substrate-1 are important for full activation of insulin-stimulated phosphatidylinositol 3-kinase activity and translocation of GLUT4 in adipose cells. *Endocrinology.* 142:2833–2840.

Franke, T.F., D.R. Kaplan, L.C. Cantley, and A. Toker. 1997. Direct regulation of the Akt proto-oncogene product by phosphatidylinositol-3,4-bisphosphate. *Science.* 275:665–668.

Fruman, D.A., R.E. Meyers, and L.C. Cantley. 1998. Phosphoinositide kinases. *Annu. Rev. Biochem.* 67:481–507.

Fruman, D.A., F. Mauvais-Jarvis, D.A. Pollard, C.M. Yballe, D. Brazil, R.T. Bronson, C.R. Kahn, and L.C. Cantley. 2000. Hypoglycaemia, liver necrosis and perinatal death in mice lacking all isoforms of phosphoinositide 3-kinase p85 alpha. *Nat. Genet.* 26:379–382.

Gillham, H., M.C. Golding, R. Pepperkok, and W.J. Gullick. 1999. Intracellular movement of green fluorescent protein–tagged phosphatidylinositol 3-kinase in response to growth factor receptor signaling. *J. Cell Biol.* 146:869–880.

Gray, A., J. Van Der Kaay, and C.P. Downes. 1999. The pleckstrin homology domains of protein kinase B and GRP1 (general receptor for phosphoinositides-1) are sensitive and selective probes for the cellular detection of phosphatidylinositol 3,4-bisphosphate and/or phosphatidylinositol 3,4,5-trisphosphate in vivo. *Biochem. J.* 344:929–936.

Griffiths, G. 1993. Fine Structure Immunocytochemistry. Springer-Verlag New York Inc., Berlin. 459 pp.

Harpur, A.G., M.J. Layton, P. Das, M.J. Bottomley, G. Panayotou, P.C. Driscoll, and M.D. Waterfield. 1999. Intermolecular interactions of the p85alpha regulatory subunit of phosphatidylinositol 3-kinase. *J. Biol. Chem.* 274:12323–12332.

Huo, H., X. Guo, S. Hong, M. Jiang, X. Liu, and K. Liao. 2003. Lipid rafts/caveolae are essential for insulin-like growth factor-1 receptor signaling during 3T3-L1 preadipocyte differentiation induction. *J. Biol. Chem.* 278:11561–11569.

Inoue, G., B. Cheatham, R. Emkey, and C.R. Kahn. 1998. Dynamics of insulin signaling in 3T3-L1 adipocytes. Differential compartmentalization and trafficking of insulin receptor substrate (IRS)-1 and IRS-2. *J. Biol. Chem.* 273:11548–11555.

James, S.R., C.P. Downes, R. Gigg, S.J. Grove, A.B. Holmes, and D.R. Alessi. 1996. Specific binding of the Akt-1 protein kinase to phosphatidylinositol 3,4,5-trisphosphate without subsequent activation. *Biochem. J.* 315:709–713.

Joly, M., A. Kazlauskas, and S. Corvera. 1995. Phosphatidylinositol 3-kinase activity is required at a postendocytic step in platelet-derived growth factor receptor trafficking. *J. Biol. Chem.* 270:13225–13230.

Jones, S.M., and A. Kazlauskas. 2001. Growth-factor-dependent mitogenesis requires two distinct phases of signalling. *Nat. Cell Biol.* 3:165–172.

Kanai, F., H. Liu, S.J. Field, H. Akbary, T. Matsuo, G.E. Brown, L.C. Cantley, and M.B. Yaffe. 2001. The PX domains of p47phox and p40phox bind to lipid products of PI(3)K. *Nat. Cell Biol.* 3:675–678.

Kirwan, J.P., A. Varastehpour, M. Jing, L. Presley, J. Shao, J.E. Friedman, and P.M. Catalano. 2004. Reversal of insulin resistance postpartum is linked to enhanced skeletal muscle insulin signaling. *J. Clin. Endocrinol. Metab.* 89:4678–4684.

Kulik, G., A. Klippel, and M.J. Weber. 1997. Antiapoptotic signalling by the insulin-like growth factor I receptor, phosphatidylinositol 3-kinase, and Akt. *Mol. Cell. Biol.* 17:1595–1606.

Li, L., L.M. Gronning, P.O. Anderson, S. Li, K. Edvardsen, J. Johnston, D. Kioussis, P.R. Shepherd, and P. Wang. 2004. Insulin induces SOCS-6 expression and its binding to p85 monomer of phosphoinositide 3-kinase, resulting in improvement in glucose metabolism. *J. Biol. Chem.* 279: 34107–34114.

Mauvais-Jarvis, F., K. Ueki, D.A. Fruman, M.F. Hirshman, K. Sakamoto, L.J. Goodyear, M. Iannacone, D. Accili, L.C. Cantley, and C.R. Kahn. 2002. Reduced expression of the murine p85alpha subunit of phosphoinositide 3-kinase improves insulin signaling and ameliorates diabetes. *J. Clin. Invest.* 109:141–149.

Nave, B.T., R.J. Haigh, A.C. Hayward, K. Siddle, and P.R. Shepherd. 1996. Compartment-specific regulation of phosphoinositide 3-kinase by platelet-derived growth factor and insulin in 3T3-L1 adipocytes. *Biochem. J.* 318:55–60.

Nolte, R.T., M.J. Eck, J. Schlessinger, S.E. Shoelson, and S.C. Harrison. 1996. Crystal structure of the PI 3-kinase p85 amino-terminal SH2 domain and its phosphopeptide complexes. *Nat. Struct. Biol.* 3:364–374.

Rameh, L.E., C.S. Chen, and L.C. Cantley. 1995. Phosphatidylinositol (3,4,5)P3 interacts with SH2 domains and modulates PI 3-kinase association with tyrosine-phosphorylated proteins. *Cell.* 83:821–830.

Rohrschneider, L.R., J.F. Fuller, I. Wolf, Y. Liu, and D.M. Lucas. 2000. Structure, function, and biology of SHIP proteins. *Genes Dev.* 14:505–520.

Rordorf-Nikolic, T., D.J. Van Horn, D. Chen, M.F. White, and J.M. Backer. 1995. Regulation of phosphatidylinositol 3′-kinase by tyrosyl phosphoproteins. Full activation requires occupancy of both SH2 domains in the 85-kDa regulatory subunit. *J. Biol. Chem.* 270:3662–3666.

Rotem-Yehudar, R., E. Galperin, and M. Horowitz. 2001. Association of insulin-like growth factor 1 receptor with EHD1 and SNAP29. *J. Biol. Chem.* 276:33054–33060.

Saltiel, A.R., and C.R. Kahn. 2001. Insulin signalling and the regulation of glucose and lipid metabolism. *Nature.* 414:799–806.

Songyang, Z., S.E. Shoelson, M. Chaudhuri, G. Gish, T. Pawson, W.G. Haser, F. King, T. Roberts, S. Ratnofsky, R.J. Lechleider, et al. 1993. SH2 domains recognize specific phosphopeptide sequences. *Cell.* 72:767–778.

Terauchi, Y., Y. Tsuji, S. Satoh, H. Minoura, K. Murakami, A. Okuno, K. Inukai, T. Asano, Y. Kaburagi, K. Ueki, et al. 1999. Increased insulin sensitivity and hypoglycaemia in mice lacking the p85 alpha subunit of phosphoinositide 3-kinase. *Nat. Genet.* 21:230–235.

Toomre, D., and D.J. Manstein. 2001. Lighting up the cell surface with evanescent wave microscopy. *Trends Cell Biol.* 11:298–303.

Tureckova, J., E.M. Wilson, J.L. Cappalonga, and P. Rotwein. 2001. Insulin-like growth factor-mediated muscle differentiation: collaboration between phosphatidylinositol 3-kinase-Akt-signaling pathways and myogenin. *J. Biol. Chem.* 276:39264–39270.

Ueki, K., P. Algenstaedt, F. Mauvais-Jarvis, and C.R. Kahn. 2000. Positive and negative regulation of phosphoinositide 3-kinase-dependent signaling pathways by three different gene products of the p85alpha regulatory subunit. *Mol. Cell. Biol.* 20:8035–8046.

Ueki, K., D.A. Fruman, S.M. Brachmann, Y.H. Tseng, L.C. Cantley, and C.R. Kahn. 2002a. Molecular balance between the regulatory and catalytic subunits of phosphoinositide 3-kinase regulates cell signaling and survival. *Mol. Cell. Biol.* 22:965–977.

Ueki, K., C.M. Yballe, S.M. Brachmann, D. Vicent, J.M. Watt, C.R. Kahn, and L.C. Cantley. 2002b. Increased insulin sensitivity in mice lacking p85beta subunit of phosphoinositide 3-kinase. *Proc. Natl. Acad. Sci. USA.* 99:419–424.

Ueki, K., D.A. Fruman, C.M. Yballe, M. Fasshauer, J. Klein, T. Asano, L.C. Cantley, and C.R. Kahn. 2003. Positive and negative roles of p85 alpha and p85 beta regulatory subunits of phosphoinositide 3-kinase in insulin signaling. *J. Biol. Chem.* 278:48453–48466.

Varnai, P., K.I. Rother, and T. Balla. 1999. Phosphatidylinositol 3-kinase-dependent membrane association of the Bruton's tyrosine kinase pleckstrin homology domain visualized in single living cells. *J. Biol. Chem.* 274:10983–10989.

Virkamaki, A., K. Ueki, and C.R. Kahn. 1999. Protein-protein interaction in insulin signaling and the molecular mechanisms of insulin resistance. *J. Clin. Invest.* 103:931–943.

White, M.F. 1998. The IRS-signaling system: a network of docking proteins that mediate insulin and cytokine action. *Recent Prog. Horm. Res.* 53:119–138.

Yu, J., C. Wjasow, and J.M. Backer. 1998a. Regulation of the p85/p110alpha phosphatidylinositol 3′-kinase. Distinct roles for the n-terminal and c-terminal SH2 domains. *J. Biol. Chem.* 273:30199–30203.

Yu, J., Y. Zhang, J. McIlroy, T. Rordorf-Nikolic, G.A. Orr, and J.M. Backer. 1998b. Regulation of the p85/p110 phosphatidylinositol 3′-kinase: stabilization and inhibition of the p110alpha catalytic subunit by the p85 regulatory subunit. *Mol. Cell. Biol.* 18:1379–1387.

Zacharias, D.A. 2002. Sticky caveats in an otherwise glowing report: oligomerizing fluorescent proteins and their use in cell biology. *Sci. STKE.* 2002:PE23.